https://doi.org/10.5194/egusphere-2026-6728
Preprint. Discussion started: 11 November 2026
© Author(s) 2026. CC BY 4.0 License.

Long-term hydroclimatic and anthropogenic drivers of Tashk-Bakhtegan endorheic lake decline

Mehraneh Seyedan[1], Milad Aminzadeh[1,2*], Matin Mir[3], Kaveh Madani[3], Nima Shokri[1,2*]

[1]Institute of Geo-Hydroinformatics, Hamburg University of Technology, Hamburg, Germany

[2]United Nations University Hub on Engineering to Face Climate Change at the Hamburg University of Technology, United Nations University Institute for Water, Environment and Health (UNU-INWEH), Hamburg, Germany

[3]United Nations University Institute for Water, Environment and Health (UNU-INWEH), Richmond Hill, Ontario, Canada

Correspondence to:

Milad Aminzadeh (milad.aminzadeh@tuhh.de)
Nima Shokri (nima.shokri@tuhh.de)

Abstract

Endorheic lakes are highly sensitive to climate variability and upstream water regulation, especially in arid and semi-arid regions. This study investigates the long-term decline of the Tashk-Bakhtegan lake system in southern Iran by integrating hydroclimatic variables, satellite-derived water extent dynamics, land cover change, and trend analysis. Results show a clear shift toward warmer and more water limited conditions in the basin during the study period from 1990 to 2024, where precipitation declined by approximately 2.0 mm yr^{-1}, while air temperature and potential evapotranspiration increased by about 0.05 °C yr^{-1} and 4.7 mm yr^{-1}, respectively. Over the same period, lake area decreased by 22.5 km^2 yr^{-1}, whereas area of human-made reservoirs slightly increased by 0.41 km^2 yr^{-1}. Land cover changes in the basin further showed surface water loss, bare land expansion, and cropland decline. Breakpoint analysis identified a major transition around 2005-2006, when increasing climatic water stress coincided with rapid lake decline and a growing contrast between natural lake area and managed reservoir surfaces. These findings demonstrate that endorheic basins are especially susceptible when warming, drying trends coincide with unregulated upstream water extraction, underscoring the need for sustainable strategies to sustain terminal lake ecosystems.

1. Introduction

The closed hydrological structure of endorheic lakes makes them exceptionally sensitive to variations in precipitation, evapotranspiration, and upstream water management and allocation. Within the past few decades, accelerated shrinkage of endorheic lakes under climate change and human pressure has emerged as a global ecological crisis, particularly across arid and semi-arid regions (Immerzeel et al., 2020; Sun et al., 2026; Tao et al., 2020; Turner et al., 2007). Declining water levels in these systems not only threaten biodiversity and disrupt ecosystem functioning, but also erode water security and livelihood for surrounding communities.

The Bakhtegan and Tashk Lakes, which are respectively the second and third largest hypersaline lakes in southern Iran, have undergone substantial desiccation in recent decades (Figure 1). Their decline has been associated with recurrent multi-year droughts which have enhanced evaporative demand and intensified upstream dam construction, agricultural water use, and

https://doi.org/10.5194/egusphere-2026-6728
Preprint. Discussion started: 11 November 2026
© Author(s) 2026. CC BY 4.0 License.

groundwater depletion (Ghader, 2018; Kabe and Rezaei, 2025; Mozafari et al., 2022). Desiccation of these lakes has put their Ramsar-listed ecosystems, which previously supported diverse migratory bird populations and unique hypersaline species, at severe risks (Ramsar Convention Secretariat, 2016; Sajedipour et al., 2017; Sayyah-Jahromi and Hatami, 2023). Beyond ecological losses, drying of Tashk and Bakhtegan lakes has also raised concerns about soil salinization, land degradation and subsidence, dust storms, and socio-environmental vulnerability across the basin (Golian et al., 2021; Haghshenas Haghighi and Motagh, 2024; Vahidipour et al., 2021).

Several studies have examined the drivers of hydrological decline of the basin. While some studies emphasize the role of climatic variability and recurrent droughts in the shrinkage of the lakes (Mirmousavi, 2024; Mohammadibigedli et al., 2022; Nasiri et al., 2023), others highlight the dominant influence of local human interventions, such as dam construction, changes in river routing, and the substantial expansion of irrigation in the upstream catchments (Bagheri et al., 2016; Kiani et al., 2017).

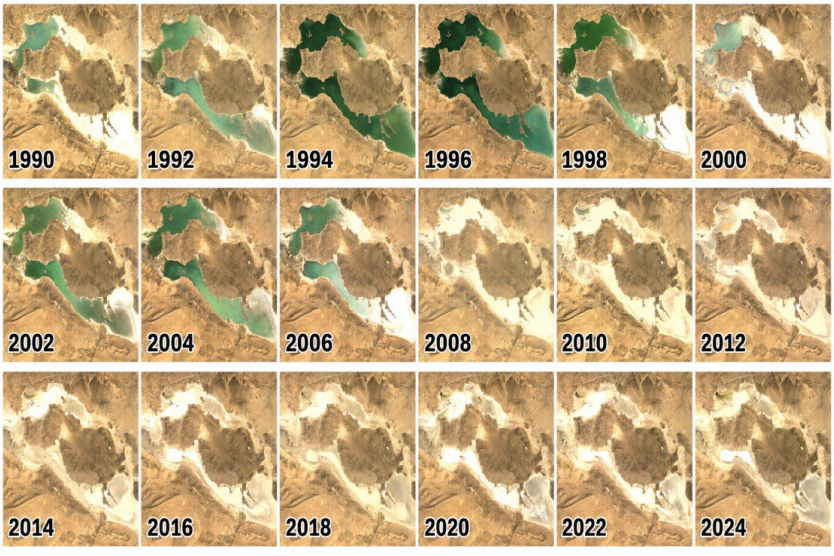


Figure 1: Annual variation of Tashk-Bakhtegan lake water extent during the study period (1990-2024).

Although these studies have provided valuable evidence on the decline of the Tashk-Bakhtegan lake system, how hydroclimatic stress together with development of water storage infrastructure and land-cover change over the past few decades contributed to the shrinkage of the lake has received less attention. In particular, distinguishing gradual climate-driven drying from a more abrupt environmental transition requires a consistent multi-indicator assessment rather than studying individual factors. Here, we integrate Earth observation and reanalysis datasets to investigate the coupled hydroclimatic, surface water, and land-cover transformations of the Tashk-Bakhtegan basin over the period 1990-2024. By investigating hydroclimatic conditions, surface water dynamics, and land-cover change, we characterize the natural and anthropogenic factors associated with the decline of the endorheic lake system and assess their implications for long-term water availability, ecosystem resilience, and regional socio-economic stability. This integrated assessment provides a basin-scale perspective on the processes underlying lake decline and the broader hydro-environmental transformation of this vulnerable endorheic system.

https://doi.org/10.5194/egusphere-2026-6728
Preprint. Discussion started: 11 November 2026
© Author(s) 2026. CC BY 4.0 License.

2. Data and Methods

2.1. Study area

The Tashk-Bakhtegan basin (Figure 2) is a closed (endorheic) drainage system in Fars Province, southern Iran (51°42′-54°31′ E; 29°00′-31°14′ N), covering approximately 27,000 km². The basin is primarily fed by the Kor and Sivand rivers, which merge downstream and terminate in the saline Tashk and Bakhtegan lakes. A smaller but hydrologically connected water body, Kaftar Lake, located in the upper-central part of the basin historically functions as an intermediate storage, influencing seasonal runoff and salinity transport within the basin. The basin has a semi-arid climate, with long-term (1960-2024) averages of 250 mm of rainfall, and a mean temperature of 14.7 °C. Elevation ranges from about 1500 m at the lakebeds to about 3900 m in the northwest where the headwaters of both rivers are located.

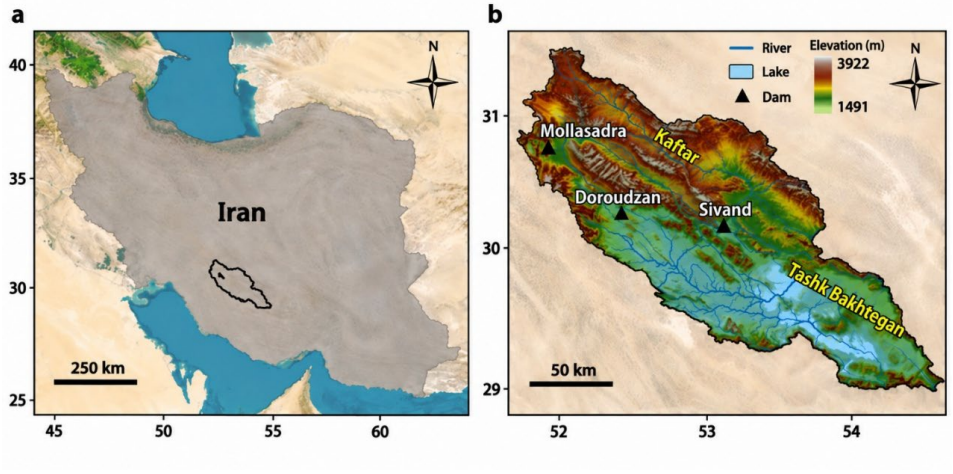


Figure 2: (a) Tashk-Bakhtegan basin in southern Iran. (b) Land elevation, lakes, rivers, and main dams within the basin.

The construction of the Doroudzan Dam with a capacity of 960 million m³ in 1972, followed by Mollasadra Dam with 440 million m³ in 2006, and Sivand Dam with 255 million m³ in 2007 (collectively storing about 1.66 billion m³), has profoundly reshaped the basin's natural flow regime and disrupted its hydrological continuity (Torabi Haghighi and Kløve, 2017; Hamidifar et al., 2022; Vahidipour et al., 2024).

2.2. Datasets

Lake and reservoir extents were derived from HydroLAKES-TopoCat v1.1, which incorporates approximately 1.43 million lake and reservoir polygons with surface areas greater than 10 ha (0.1 km²), based on the HydroLAKES v1.0 inventory (Messager et al., 2016). River networks were extracted from HydroRIVERS v10, a globally consistent vector hydrography dataset at ~500 m resolution (Lehner and Grill, 2013). Dam locations and reservoir footprints were obtained from Global Dam Watch v1.0, comprising 35,295 global reservoirs with associated structural and operational metadata (Lehner et al., 2024). These layers were visually inspected and corrected where necessary in ArcGIS to improve shoreline representation and avoid omission of marginal water pixels, before being imported into Google Earth Engine for spatial analysis, annual area calculation, and time-series extraction.

https://doi.org/10.5194/egusphere-2026-6728
Preprint. Discussion started: 11 November 2026
© Author(s) 2026. CC BY 4.0 License.

Surface water dynamics were then quantified using the JRC Global Surface Water dataset at 30 m spatial resolution (Pekel et al., 2016). The analysis focused on the natural lakes of the basin, including Bakhtegan, Tashk, and Kaftar, as well as the major human-made reservoirs, including the Doroudzan, Mollasadra, and Sivand dams. To reduce uncertainties associated with limited image availability, sensor differences, and radiometric inconsistencies in the early Landsat records, the analysis was restricted to 1990-2024, a period characterized by more consistent Landsat observations and improved spatial and temporal coverage (Wulder et al., 2019). For each year, the annual GSW waterClass layer was extracted and clipped to the boundaries described above, and the corresponding annual surface water area was calculated in Google Earth Engine for each lake and reservoir.

Hydroclimatic variables, including daily precipitation, 2-m air temperature, and actual and potential evapotranspiration, were obtained from the ERA5-Land reanalysis dataset from 1950 to present at ~9 km spatial resolution (Muñoz-Sabater et al., 2021). Actual evapotranspiration was included as a combined land-climate response variable. SPEI-z was derived from annual precipitation and potential evapotranspiration to represent standardized climatic water balance stress. For the SPEI-z calculation, annual climatic water balance was first defined as (P − PET) and then standardized pixel-wise relative to the 1950-2024 baseline, using the long-term mean and standard deviation of each pixel. Basin-scale annual SPEI-z values were obtained by spatially averaging the standardized pixel-level values within the Tashk-Bakhtegan basin.

Land cover trajectories were reconstructed from GLC_FCS30D, a 30 m global annual land cover time series (1985-2022) derived from dense Landsat archives and continuous change detection (Zhang et al., 2024). Because the dataset provides land-cover information at five-year intervals before 2000, the analysis was restricted to the period 2000-2022. We focused on surface water, cropland, and bare land, which are particularly relevant to the basin's hydrological transition.

To assess atmospheric dust activity, the Sentinel-5P TROPOMI Absorbing Aerosol Index (AAI) was employed, a UV-based indicator of light-absorbing aerosols such as mineral dust and smoke. The index is derived from differences between measured and modeled UV reflectance, with positive values indicating the presence and relative strength of UV-absorbing aerosols, while near-zero or negative values are generally associated with weakly absorbing or non-absorbing aerosols or clouds. This dataset provides daily global coverage and is well suited for detecting dust plumes over bright land surfaces. All scenes intersecting the Tashk-Bakhtegan basin were extracted in Google Earth Engine, and annual composites were generated to derive the frequency of dust occurrence.

2.3. Trend and breakpoint analysis

We analyzed long-term hydrological trends within the basin using least-squares linear regression which provided annual rates of shrinkage or expansion for the water bodies. Additionally, abrupt shifts were identified using two single-breakpoint homogeneity tests: the Buishand range test, and the standard normal homogeneity test (SNHT). The Buishand test is based on cumulative deviations from the mean and is widely used to assess shifts in hydroclimatic records such as precipitation and other hydrological time series (Buishand, 1982). The adjusted partial sum, S_k, is defined as:

$$S_k = \sum_{i=1}^{k}(y_i - \overline{y}) \quad (1)$$

where y_i is the observed value of the hydrological variable in the year i, $\overline{y}$ is the arithmetic mean of all n observations in the time series, i is the observation index, $k = 1, \ldots, n$, and $S_0 = 0$.

https://doi.org/10.5194/egusphere-2026-6728
Preprint. Discussion started: 11 November 2026
© Author(s) 2026. CC BY 4.0 License.

When the series is homogeneous, S_k fluctuates around zero. A break is indicated in the year y where S_k reaches a maximum (a negative shift) or a minimum (a positive shift). The rescaled adjusted range, R, is then obtained as:

$$R = \frac{\max(S_k) - \min(S_k)}{D_y} \quad (2)$$

where D_y is the sample standard deviation of the y series. The statistic $R/\sqrt{n}$ is then compared with the critical values tabulated by Buishand (1982).

The SNHT test compares the mean of the first y years of a series with the mean of the remaining ($n-y$) years (Alexandersson, 1986):

$$T_y = y\bar{z}_1^2 + (n-y)\bar{z}_2^2, \quad y = 1, 2, \ldots, n \quad (3)$$

where $\bar{z}_1$ and $\bar{z}_2$ are the means of the standardized values for each of the two subperiods, respectively:

$$\bar{z}_1 = \frac{1}{y}\sum_{i=1}^{y}\frac{y_i - \bar{y}}{s} \quad (4)$$

$$\bar{z}_2 = \frac{1}{n-y}\sum_{i=y+1}^{n}\frac{y_i - \bar{y}}{s} \quad (5)$$

where $\bar{y}$ and s are the mean and standard deviation of the complete series, respectively. The most probable break year is the value of y that maximizes T_y. H_0 (homogeneity) is rejected in favor of H_1 (a break at year y) if $T_0 = \max_{0 \le y \le n} T_y$ exceeds the critical value for a chosen significance level, which depends on the sample size n (Alexandersson, 1986). Note that detected breakpoints indicate potential statistical shifts and do not, by themselves, establish the underlying hydrological causes.

3. Results

3.1. Lake and reservoir surface water dynamics

Variations in the surface areas of lake and human-made reservoirs during the study period are shown in Figure 3. Although the sharp decline in lake area in the early 2000s was initially accompanied by a decrease in reservoir area, Figure 3a reveals a contrasting pattern beginning in 2006. Despite a decrease in lake extent, reservoir surface area increased substantially, marking the onset of a shift in the reservoir to lake area ratio (Figure 3b).

To test this shift, the annual lake surface area series (1990-2024) was examined for abrupt changes using the SNHT and the Buishand range test described in Section 2.3. Both tests independently identified a statistically significant breakpoint at the 2005/2006 transition ($p < 0.05$). We thus divided the study period into two intervals, 1990-2005 and 2006-2024, to assess temporal trends and changes in hydroclimatic parameters. Mean lake surface area declined from 503.4 km² during 1990-2005 to 37.4 km² during 2006-2024, a reduction of about 92.6%. The magnitude and persistence of this difference are consistent with the abrupt shift identified by the breakpoint tests, rather than short-term interannual variability. Over the 1990-2024 record, lake surface area declined at an average rate of approximately 22.5 km² yr⁻¹. In contrast, surface area of reservoirs followed an opposing trajectory, increasing from a mean of about 31.5 km² during 1990-2005 to about 39.6 km² during 2006-2024, an increase of roughly 26% (Figure 3a). Over the full study period, reservoir surface area exhibited a positive linear trend of ~ 0.41 km² yr⁻¹.

https://doi.org/10.5194/egusphere-2026-6728
Preprint. Discussion started: 11 November 2026
© Author(s) 2026. CC BY 4.0 License.

The timing of this transition is hydrologically meaningful in the context of upstream regulation. The basin had already been regulated by Doroudzan Dam since 1972, with a storage capacity of approximately 960 million m³. The operation of two additional major upstream reservoirs, Mollasadra Dam in 2006 and Sivand Dam in 2007, added substantial regulated storage during the same period when lake decline became more persistent. Together, these three reservoirs represent about 1.66 billion m³ of upstream storage capacity, indicating a growing imbalance between shrinking natural terminal water bodies and expanding regulated upstream storage after 2006. It suggests a broader hydrological transformation in which surface water was increasingly retained and regulated upstream, while the downstream terminal lakes experienced persistent desiccation.

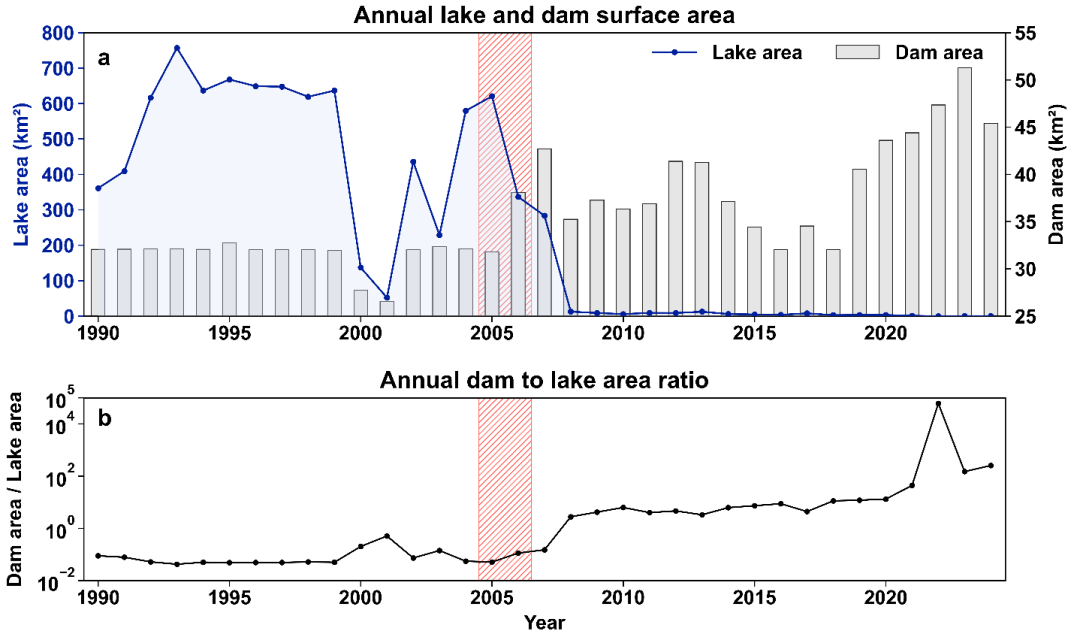


Figure 3: (a) Annual variations in lake and dam surface areas in the Tashk-Bakhtegan Basin during 1990-2024. (b) Annual dams to lakes area ratio (%). The red hatched area indicates the 2005/2006 transition period.

3.2. Spatio-temporal assessment of climate variability and drought stress

Spatial variations in precipitation, temperature, and actual and potential evapotranspiration across the basin are depicted in Figure 4. The spatial pattern of precipitation (Figure 4a) shows a clear and progressive drying across the basin. During 1990-2005, mean annual precipitation ranged from ~140 to 760 mm yr⁻¹, shaped strongly by the orographic gradient between the Zagros Mountains in the northwest and the terminal drainage area in the southeast. This spatial pattern persisted from 2006 to 2024, but at notably lower values, ranging from 118 to 636 mm yr⁻¹, as the basin experienced a mean reduction of about 54.8 mm yr⁻¹ between the two periods. The spatial difference map highlights a more intense signal in the northwestern highlands, where reductions reach up to 150 mm yr⁻¹. These areas historically supplied substantial runoff to Tashk and Bakhtegan Lakes, and their pronounced drying further constrains downstream water availability.

Temperature patterns in Figure 4b indicate a clear warming between the two periods. During 1990-2005, mean annual temperatures ranged from approximately 8.5 °C in the upland areas to about 20.1 °C in the lower basin. In 2006-2024, temperatures increased by roughly 0.8 °C across most of the basin, with the strongest warming concentrated mainly in the western-central part of the basin,

https://doi.org/10.5194/egusphere-2026-6728
Preprint. Discussion started: 11 November 2026
© Author(s) 2026. CC BY 4.0 License.

while the eastern and southeastern sectors showed comparatively smaller increases. This warming enhances atmospheric evaporative demand and thus accelerates soil moisture and lake water loss.

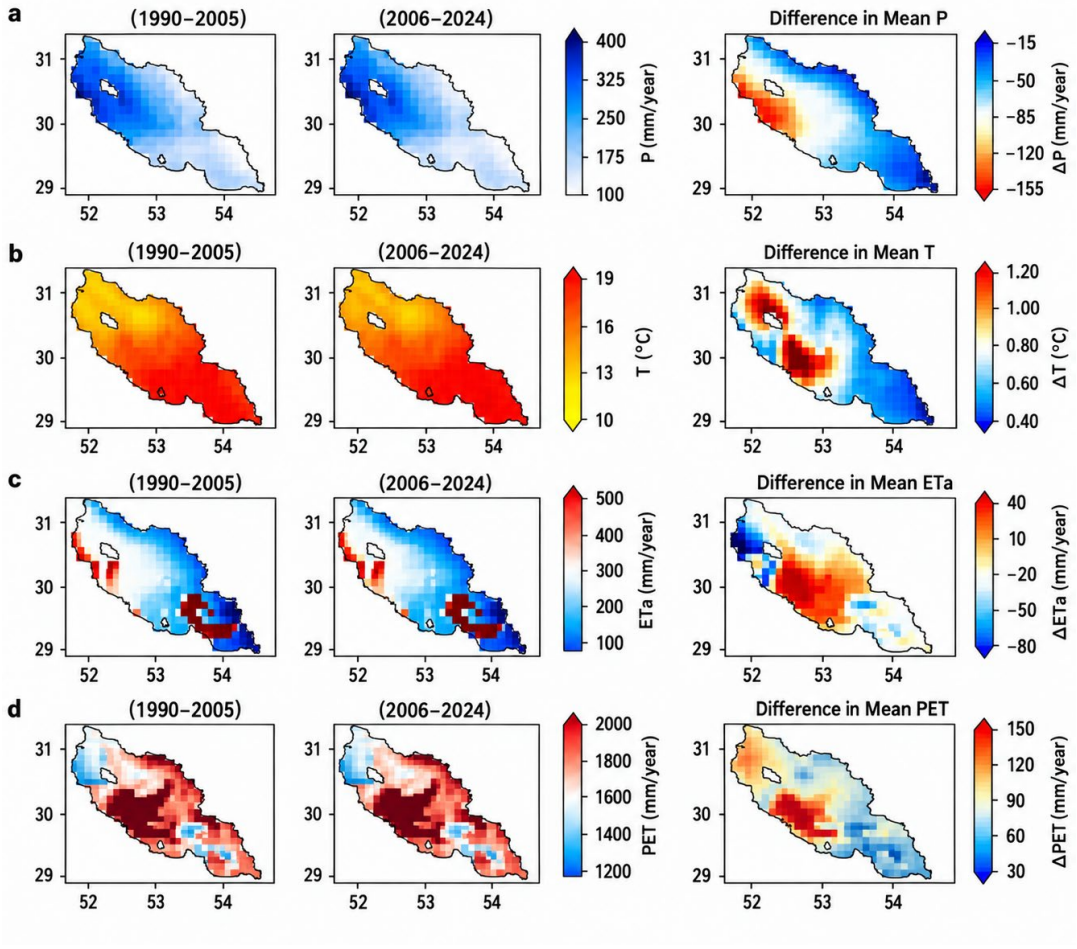


Figure 4: Spatial variation of hydroclimatic parameters (1990-2024) within the Tashk-Bakhtegan basin. Mean precipitation (a), temperature (b), actual evapotranspiration (c), and potential evapotranspiration (d) for 1990-2005 and 2006-2024, and their corresponding differences between these two periods.

Actual evapotranspiration (ET_a) shows strong spatial variations across the basin (Figure 4c). During 1990-2005, the highest ET_a values equal to 1264 mm yr^{-1} occurred over Tashk-Bakhtegan Lakes, followed by reservoirs, croplands, and vegetated foothills, while the dry and cold uplands exhibited the lowest rates. Between 2006 and 2024, ET_a declined sharply, by 40–75 mm yr^{-1}, across the northwestern uplands and over the lake and its adjacent lands as the lakes desiccated. In contrast, ET_a increased modestly (up to ~40 mm yr^{-1}) across large portions of the cropland-dominated southern and western plains (see Figure 7b).

Potential evapotranspiration (PET) patterns (Figure 4d) indicate a clear increase between the two periods. During 1990-2005, mean annual PET ranged from about 1253 to 2503 mm yr^{-1}, with the lowest values in the colder northwestern uplands and the highest across the central, eastern, and southern lowlands. In 2006-2024, PET increased to a range of about 1285-2684 mm yr^{-1}, while the overall spatial gradient remained similar. The difference map shows a basin-wide increase of about 30-192 mm yr^{-1}, with the

https://doi.org/10.5194/egusphere-2026-6728
Preprint. Discussion started: 11 November 2026
© Author(s) 2026. CC BY 4.0 License.

strongest increases concentrated in the central-western and south-central plains. This widespread rise in PET indicates intensified atmospheric evaporative demand under warmer conditions, potentially increasing soil moisture depletion, irrigation demand, and adding further pressure on the limited water resources of the basin.

The temporal patterns of precipitation, temperature, and actual and potential evapotranspiration in Figure 5 provide additional evidence of long-term hydroclimatic change within the basin. Precipitation anomalies fluctuate widely, between about -127 and +262 mm, reflecting the basin's substantial interannual variability. Despite this variability, the long-term trend is negative, at about -1.6 mm yr^{-1}, and median precipitation was approximately 33 mm yr^{-1} lower during 2006-2024 than during 1990-2005 (Figure 5a, boxplots), consistent with a sustained drying trend.

Temperature anomalies show a much clearer, monotonic trend (Figure 5b). From the mid-1990s onward, nearly all years show positive anomalies relative to the 1960-1990 baseline, with a linear increase of roughly +0.05 °C yr^{-1}. The rise in temperature over the 34-year record is about +1.8 °C, with individual years such as 2021 and 2010 reaching anomalies of up to +2.4 °C, reshaping atmospheric evaporative demand and intensifying surface-water losses. The corresponding boxplots show a higher average temperature and a greater frequency of warm years.

ET_a anomalies show more complex behavior, reflecting the interplay between atmospheric evaporative demand and water availability (Figure 5c). ET_a anomalies vary between about -53 and +104 mm, and the long-term trend is only slightly negative (roughly -0.3 mm yr^{-1}). Despite rising temperatures across the basin, this modest decline in ET_a coincides with the shrinkage of the lakes and wetlands that previously sustained high evaporative losses where median ET_a decreased by roughly 25 mm in the second period relative to the first. The boxplots illustrate this transition, showing a downward shift in median ET_a and a greater frequency of low-ET_a years that align with the basin's most severe drought years and with the period of lake desiccation.

Potential evapotranspiration anomalies show a clear, persistent increasing trend over the study period (Figure 5d). PET anomalies vary between about -150 and +150 mm relative to the 1960-1990 mean of 1767.3 mm, with predominantly negative anomalies during the 1990s and early 2000s. From about 2007 onward, most years show positive anomalies, and the long-term trend is an increase of about +4.7 mm yr^{-1}, consistent with the basin-wide PET trend reported above. The highest positive anomalies occur during the late 2010s and in 2021, reflecting a progressive intensification of atmospheric evaporative demand. The corresponding boxplots show a pronounced upward shift between the two periods, with median PET increasing by approximately 76 mm from 1990-2005 to 2006-2024. Together with the observed warming, this rise in PET points to greater potential water loss and intensifying water stress across the basin.

https://doi.org/10.5194/egusphere-2026-6728
Preprint. Discussion started: 11 November 2026
© Author(s) 2026. CC BY 4.0 License.

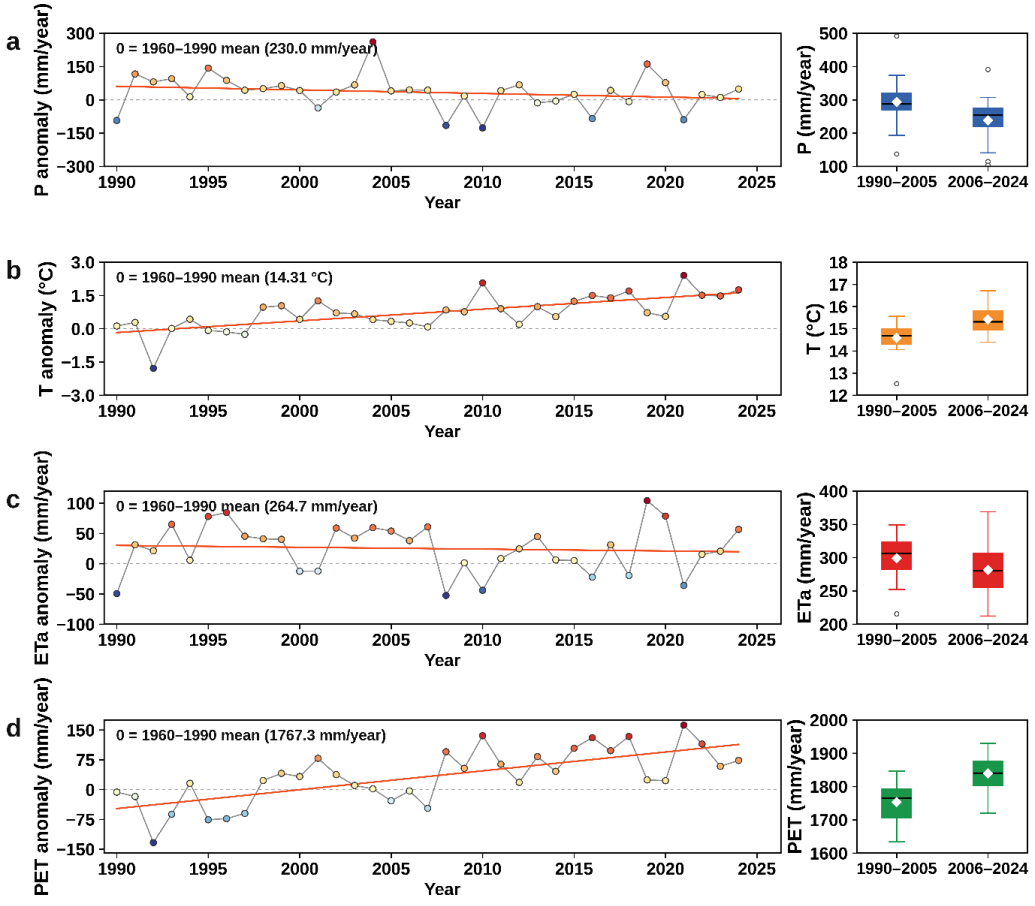


Figure 5: Temporal variability of hydroclimatic parameters (1990-2024). Anomalies and boxplots of precipitation (a), temperature (b), actual evapotranspiration (c), and potential evapotranspiration (d) for 1990-2005 and 2006-2024.

SPEI-z values show a pronounced shift toward drier conditions over the study period (Figure 6). Annual basin-mean SPEI-z values range from approximately -2.0 to +2.0, indicating substantial interannual variability between wet and dry years. During 1990-2005, most years exhibit positive values, with particularly wet conditions occurring in the mid-1990s and 2004. In contrast, negative values become more frequent and persistent after 2006, including severe to extreme drought conditions in 2008, 2010, 2016, and 2021, when SPEI-z values fell to -1.5 or below, with 2010 (-2.02) reaching the extreme drought threshold (SPEI-z ≤ -2.0). The long-term linear trend over 1990-2024 is approximately -0.05 yr^{-1}, consistent with a sustained drying trend in the basin's climatic water balance. The repeated occurrence of moderate, severe, and now also extreme droughts indicates a sustained deterioration in basin water balance. The corresponding boxplots show a clear downward shift between the two periods, with the median SPEI-z decreasing from approximately +0.5 during 1990-2005 to around -0.4 during 2006-2024. The wider lower tail in the second period further indicates an increased frequency and intensity of dry years, consistent with declining precipitation, rising temperature, and increasing potential evapotranspiration across the basin.

https://doi.org/10.5194/egusphere-2026-6728
Preprint. Discussion started: 11 November 2026
© Author(s) 2026. CC BY 4.0 License.

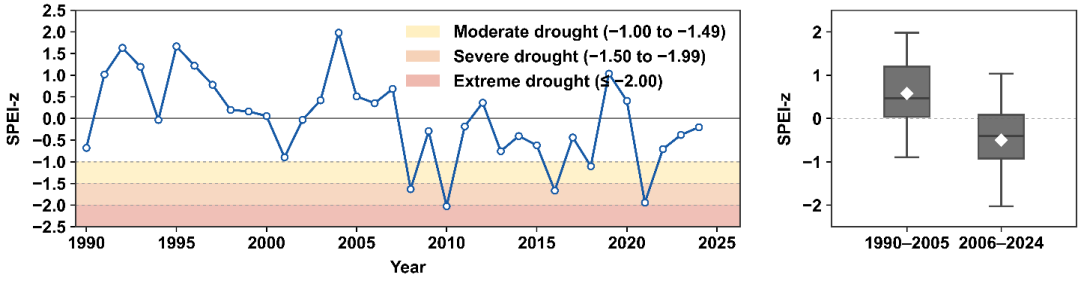


Figure 6: Annual basin-mean SPEI-z from 1990–2024 and comparison of SPEI-z distributions between 1990–2005 and 2006–2024.

3.3. Land cover change dynamics

Land cover changes provide additional evidence that the decline of the Tashk-Bakhtegan lake system was accompanied by broader landscape transformation. Figure 7 shows that between 2000 and 2022, the mapped surface water declined at an average rate of approximately 17.5 km² yr⁻¹, consistent with the contraction of lake area identified in the surface water analysis (22.5 km² yr⁻¹ from 1990 to 2024). The spatial maps show that this decline was concentrated mainly around the Tashk and Bakhtegan lake margins, where formerly inundated or seasonally wet surfaces became progressively exposed after the mid-2000s.

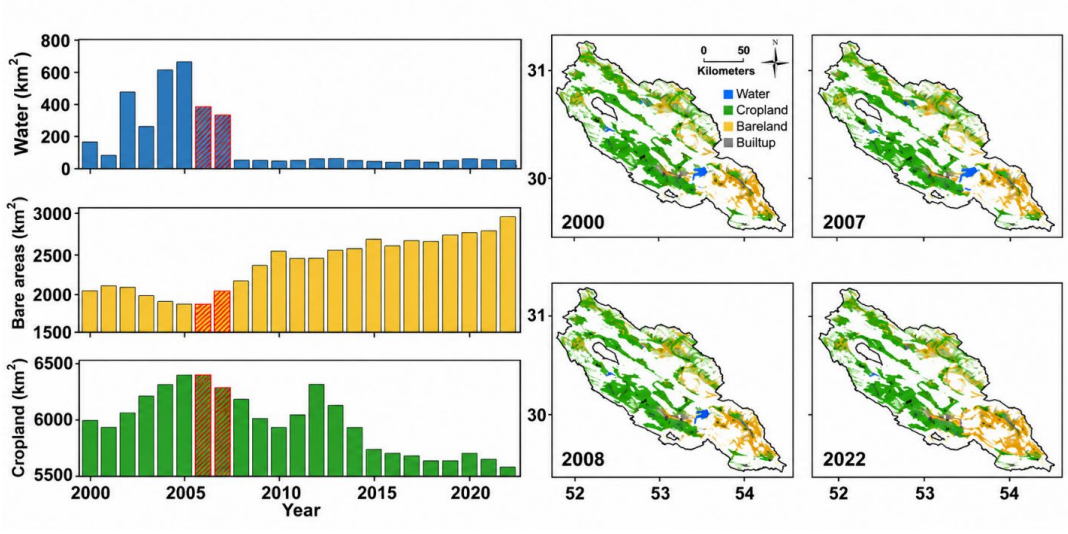


Figure 7: Land cover change dynamics (2000-2022). (a) Temporal variation of surface water, cropland, and bare area with hatched bars marking the years of Mollasadra and Sivand dam commissioning (2006-2007). (b) Land cover maps for 2000, 2007, 2008, and 2022.

The strongest land cover response was the expansion of bare land, which increased by approximately 45.9 km² yr⁻¹ during 2000-2022. This expansion was most evident around the former lakebeds and adjacent lowland areas, indicating a transition from open water and wet surfaces toward exposed dryland. The selected maps for 2000, 2007, 2008, and 2022 show that bare land expansion closely followed the areas where surface water loss was most pronounced. Cropland showed a net decline of approximately 31.3 km² yr⁻¹ during 2000-2022, indicating a gradual reduction in total mapped agricultural land within the basin. Despite the overall decline, substantial cropland areas persisted throughout the study period, particularly in the central and upstream parts of the basin. This persistence is important because continued agricultural activity requires sustained water supply in a system where surface

https://doi.org/10.5194/egusphere-2026-6728
Preprint. Discussion started: 11 November 2026
© Author(s) 2026. CC BY 4.0 License.

water availability was substantially reduced. Overall, the land cover results reveal a clear transition landscape response, characterized by surface water loss, expansion of exposed bare surfaces, and gradual reduction of total mapped cropland.

4. Discussion

4.1. Combined effects of climate and anthropogenic pressures on lake desiccation

The results indicate that the Tashk-Bakhtegan basin underwent a marked hydro-environmental transition during the mid-2000s. This transition was not limited to declining precipitation, but involved a coupled shift toward higher atmospheric evaporative demand, more negative climatic water balance conditions, contraction of natural surface water bodies, and exposure of former lakebed surfaces. Such combined hydroclimatic stress is consistent with broader evidence of increasing drought pressure and water scarcity across Iran and Southwest Asia (AghaKouchak et al., 2015; Dehghani et al., 2020; Madani, 2014).

The persistent shift in lake area identified above coincides with the operation of Mollasadra Dam in 2006 and Sivand Dam in 2007, following the earlier regulation of the basin by Doroudzan Dam since 1972. This temporal concurrence suggests that changes in water storage and regulation may have contributed to reduced downstream water availability, intensifying lake desiccation and contributing to land degradation in the basin. These findings are consistent with previous reports of the effects of water storage infrastructure on downstream hydrological conditions (Fars Regional Water & Wastewater Company, 2025; Sayyah-Jahromi and Hatami, 2023). The strong decline in lake area and total surface water extent, together with the increasing reservoir to lake area ratio, therefore indicates a changed surface water configuration in which regulated upstream storage remained comparatively persistent while natural terminal lakes contracted. Similar interactions between drought, water resource management, and reduced lake inflow have been reported for Lake Urmia (AghaKouchak et al., 2015; Shadkam et al., 2016).

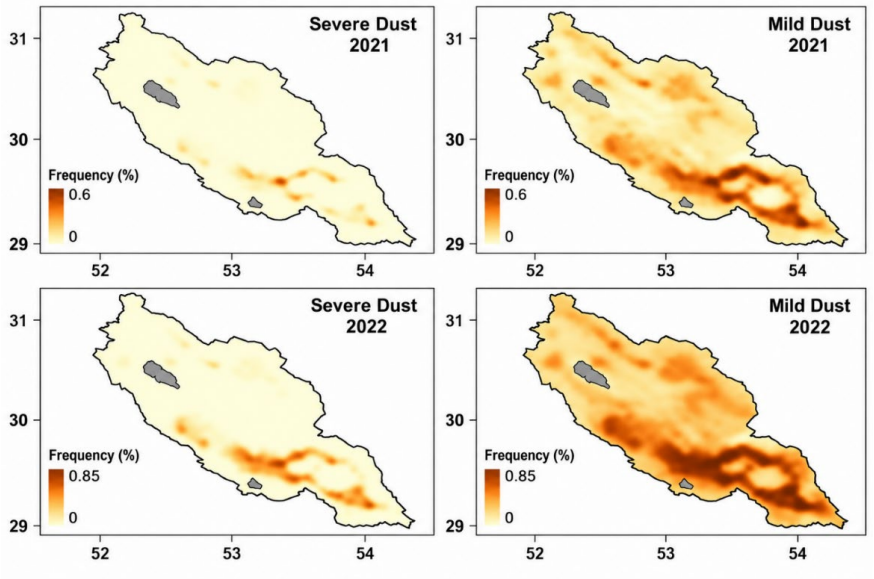
Overall, the notable decline in lake extent after 2006 is best interpreted as a coupled climatic-anthropogenic response. Climatic drying and rising evaporative demand reduced natural water availability, while upstream regulation, groundwater abstraction, and agricultural water use exerted additional pressure on downstream water availability and may have reduced the resilience of the lake system during dry years. This is consistent with previous basin scale studies that emphasized the combined roles of drought, river flow alteration, reservoir operation, groundwater depletion, and agricultural water use in the decline of the Tashk-Bakhtegan system (Mozafari et al., 2022; Kabe and Rezaei, 2025).

4.2. Environmental implications of lake desiccation

The environmental consequences of the Tashk-Bakhtegan decline extend beyond the loss of open water. Surface water contraction was accompanied by substantial bare land expansion along former lake margins and exposed lakebeds, indicating a transition from wet surfaces to dry terrain. The loss of wetland and open water surfaces may also alter local surface energy balance conditions by reducing evaporative cooling and increasing land surface temperatures around the desiccated lakes (Kim, 1992; Aminzadeh et al., 2023). This transformation is particularly important because the basin lies within the dust prone belt of Southwest Asia, where aridity and regional atmospheric circulation already favour dust mobilization and transport (Rashki et al., 2021). Lake desiccation may therefore intensify an existing regional hazard by exposing additional fine grained and saline sediments to wind erosion. Consistent with this interpretation, Figure 8 shows higher frequencies of both mild and severe dust activity in 2022 relative to 2021, particularly across the southern and southeastern parts of the basin where extensive lake desiccation and bare land expansion occurred. Although the two-year comparison does not provide definitive source attribution, the spatial correspondence between

https://doi.org/10.5194/egusphere-2026-6728
Preprint. Discussion started: 11 November 2026
© Author(s) 2026. CC BY 4.0 License.

275 exposed surfaces and enhanced dust activity supports a plausible pathway linking lakebed exposure to increased sediment availability and dust generation. Similar degradation processes have been reported for the Aral Sea and other desiccated wetlands (Hamzehpour et al., 2022; Hassani et al., 2021), while the associated salinization may further contribute to land degradation in water stressed agricultural landscapes (Shokri et al., 2024).



280 **Figure 8: Annual dust frequency maps for 2021 and 2022 showing mild and severe dust activity across the Tashk-Bakhtegan Basin.**

Groundwater decline may further intensify these risks. Although groundwater dynamics were not directly analysed in the present study, Mozafari et al. (2022) reported a basin average groundwater level decline of approximately 0.9 m yr^{-1} across the Bakhtegan basin. Such depletion can reduce aquifer storage, weaken surface water-groundwater interactions, and limit the basin's capacity to buffer dry years. In endorheic basins, declining surface water, groundwater depletion, and salinity accumulation may reinforce one
285 another, which is consistent with reported salinity concerns in the Tashk-Bakhtegan system (Vahidipour et al., 2021). Continued groundwater stress can also increase the likelihood of land subsidence and aquifer system compaction, a process widely documented in groundwater depleted regions (Galloway and Burbey, 2011; Davydzenka et al., 2024).

The expansion of exposed surfaces also has implications for land degradation and wetland habitat loss. Previous studies have reported subsidence and land degradation in Fars Province and nearby agricultural areas, particularly where groundwater extraction
290 has exceeded natural recharge (Golian et al., 2021; Haghshenas Haghighi and Motagh, 2024). Tashk and Bakhtegan lakes have historically supported Ramsar listed wetland habitats and migratory bird populations; therefore, reductions in open water and seasonally wet areas may reduce habitat availability for wetland dependent species (Ramsar Convention Secretariat, 2016; Sajedipour et al., 2017; Sayyah-Jahromi and Hatami, 2023). The observed surface water loss and bare land expansion indicate a transition toward a more exposed and degradation prone terminal basin, with potential implications for surface warming,
295 salinization, wind erosion, groundwater stress, land subsidence, land degradation, and wetland habitat loss.

https://doi.org/10.5194/egusphere-2026-6728
Preprint. Discussion started: 11 November 2026
© Author(s) 2026. CC BY 4.0 License.

4.3. Limitations and future research perspectives

Although this study systematically investigated long-term impacts of climatic and anthropogenic pressures on the desiccation of Tashk-Bakhtegan lakes, certain methodological limitations should be considered when interpreting the results. The hydroclimatic analysis relies on ERA5-Land reanalysis data, which provides spatially continuous long-term coverage but may contain biases in complex terrain. This is particularly relevant for the Tashk-Bakhtegan basin, where the northwestern highlands play an important role in runoff generation. The land cover analysis is also subject to classification uncertainty, particularly for agricultural subclasses. Although the GLC_FCS30D product includes irrigated and rainfed cropland categories, the subclass level outputs were not sufficiently consistent for reliable quantitative interpretation in the basin. To avoid overinterpreting uncertain subclass classifications, irrigated and rainfed cropland classes were aggregated and analyzed as total mapped cropland. Future studies should examine irrigation expansion in greater detail to better distinguish the influence of upstream water management and agricultural water use on the desiccation of the Tashk-Bakhtegan lake. Given the lack of reliable, detailed data on river inflows, groundwater exchanges, water withdrawals, and reservoir operations, a complete quantitative water balance reconstruction was not feasible in this study. Although the integrated hydroclimatic indicators, surface water dynamics, and trend analyses provide complementary evidence of basin scale hydrological changes, they do not allow for a quantitative separation of the relative contributions of climatic variability and human water management to lake desiccation. Future studies incorporating comprehensive hydrological data are needed to quantify these contributions more precisely.

5. Conclusion

This study provides an integrated assessment of the long-term decline of the Tashk-Bakhtegan lake system by linking hydroclimatic variability, surface water dynamics, reservoir development, and land cover change. The results show that the basin has shifted toward warmer and more water limited conditions during 1990-2024, characterized by declining precipitation, increasing temperature and PET, and more frequent negative SPEI-z values. Breakpoint analysis identified a major hydro-environmental transition around 2005/2006, after which lake shrinkage became more persistent and the contrast between natural terminal lakes and managed upstream reservoir surfaces increased. The observed decline of lake extent appears to reflect the combined influence of climatic and anthropogenic pressures, with the operation of additional major reservoirs in the mid-2000s suggesting that upstream regulation may have increased the vulnerability of the terminal lakes under already stressed climatic conditions. These changes indicate a shift toward a drier, more exposed, and more degraded system.

Overall, the Tashk-Bakhtegan basin illustrates the high sensitivity of endorheic lake systems to interacting climatic and human pressures. Future basin management should therefore prioritize environmental flow requirements, groundwater regulation, demand management, and adaptation to increasing evaporative stress under a warmer and drier climate.

Data Availability

Climatic variables including daily precipitation, air temperature, and actual evapotranspiration were obtained from the ERA5-Land reanalysis dataset (https://doi.org/10.5194/essd-13-4349-2021). Surface-water dynamics were derived from the Global Surface Water dataset (Pekel et al., 2017), accessed via Google Earth Engine. Annual land-cover information was obtained from the GLC_FCS30D global land-cover time series (https://doi.org/10.5281/zenodo.8239305). Hydrographic data on lakes and reservoirs were sourced from the HydroLAKES database (https://doi.org/10.1038/ncomms13603) and the Global Dam Watch database (https://www.globaldamwatch.org/database), while river networks were obtained from the HydroRIVERS dataset

https://doi.org/10.5194/egusphere-2026-6728
Preprint. Discussion started: 11 November 2026
© Author(s) 2026. CC BY 4.0 License.

(https://doi.org/10.1002/hyp.9740). Atmospheric aerosol and dust activity were assessed using the Sentinel-5P TROPOMI Absorbing Aerosol Index (AAI) product (https://developers.google.com/earth-engine/datasets/catalog/COPERNICUS_S5P_OFFL_L3_AER_AI). The Google Earth Engine scripts and all the necessary codes for reproducing the main results are available via https://github.com/SMehranehS/TUHH_GHI.git

Author Contributions

MS, MA, and NS contributed to conceptualization and methodology. MS carried out the analyses and wrote the original draft. MA and NS contributed to validation, investigation, and supervision. All authors contributed to interpretation of the findings and to review and editing of the manuscript.

Competing interests

The authors declare no competing interests.

Acknowledgments

The authors gratefully acknowledge the funding and resources provided by the Institute of Geo-hydroinformatics at Hamburg University of Technology. During the preparation of this work, ChatGPT was used for language editing. After using this tool, the authors reviewed and edited the content as needed and take full responsibility for the final publication.

References

AghaKouchak, A., Norouzi, H., Madani, K., Mirchi, A., Azarderakhsh, M., Nazemi, A., Nasrollahi, N., Farahmand, A., Mehran, A., Hasanzadeh, E., 2015. Aral Sea syndrome desiccates Lake Urmia: Call for action. Journal of Great Lakes Research 41, 307–311. https://doi.org/10.1016/j.jglr.2014.12.007

Aminzadeh, M., Or, D., Stevens, B., AghaKouchak, A., Shokri, N., 2023. Upper Bounds of Maximum Land Surface Temperatures in a Warming Climate and Limits to Plant Growth. Earth's Future 11, e2023EF003755. https://doi.org/10.1029/2023EF003755

Bagheri, M., Bagheri, A. and Sohooli, G.A., 2016. Analysis of changes in the Bakhtegan Lake water body under the influence of natural and human factors. Iran-Water Resources Research, 12(3), pp.1–11.

Buishand, T. A. (1982). Some methods for testing the homogeneity of rainfall records. *Journal of Hydrology, 58*(1–2), 11–27. DOI: 10.1016/0022-1694(82)90066-X

Davydzenka, T., Tahmasebi, P., Shokri, N., 2024. Unveiling the Global Extent of Land Subsidence: The Sinking Crisis. Geophysical Research Letters 51, e2023GL104497. https://doi.org/10.1029/2023GL104497

Dehghani, M., Salehi, S., Mosavi, A., Nabipour, N., Shamshirband, S., Ghamisi, P., 2020. Spatial Analysis of Seasonal Precipitation over Iran: Co-Variation with Climate Indices. https://doi.org/10.48550/ARXIV.2001.09757

Fars Regional Water & Wastewater Company, 2025. Annual water resources report.

Galloway, D.L., Burbey, T.J., 2011. Review: Regional land subsidence accompanying groundwater extraction. Hydrogeol J 19, 1459–1486. https://doi.org/10.1007/s10040-011-0775-5

Ghader, F., 2018. Water and water shortage in Iran case study Tashk-Bakhtegan and Maharlu lakes basin, Fars Province, South Iran.

https://doi.org/10.5194/egusphere-2026-6728
Preprint. Discussion started: 11 November 2026
© Author(s) 2026. CC BY 4.0 License.

Golian, M., Saffarzadeh, A., Katibeh, H., Mahdad, M., Saadat, H., Khazaei, M., Sametzadeh, E., Ahmadi, A., Sharifi Teshnizi, E., Samadi Darafshani, M., Dashti Barmaki, M., 2021. Consequences of groundwater overexploitation on land subsidence in Fars Province of Iran and its mitigation management programme. Water & Environment J 35, 975–985. https://doi.org/10.1111/wej.12688

Haghshenas Haghighi, M., Motagh, M., 2024. Uncovering the impacts of depleting aquifers: A remote sensing analysis of land subsidence in Iran. Sci. Adv. 10, eadk3039. https://doi.org/10.1126/sciadv.adk3039

Hamidifar, H., Akbari, F., & Rowiński, P. M. (2022). Assessment of environmental water requirement allocation in anthropogenic rivers with a hydropower dam using hydrologically based methods—Case study. Water, 14(6), 893. https://doi.org/10.3390/w14060893

Hamzehpour, N., Marcolli, C., Klumpp, K., Thöny, D., Peter, T., 2022. The Urmia playa as a source of airborne dust and ice-nucleating particles – Part 2: Unraveling the relationship between soil dust composition and ice nucleation activity. Atmos. Chem. Phys. 22, 14931–14956. https://doi.org/10.5194/acp-22-14931-2022

Hassani, A., Azapagic, A., Shokri, N., 2021. Global predictions of primary soil salinization under changing climate in the 21st century. Nat Commun 12, 6663. https://doi.org/10.1038/s41467-021-26907-3

Immerzeel, W.W., Lutz, A.F., Andrade, M., Bahl, A., Biemans, H., Bolch, T., Hyde, S., Brumby, S., Davies, B.J., Elmore, A.C., Emmer, A., Feng, M., Fernández, A., Haritashya, U., Kargel, J.S., Koppes, M., Kraaijenbrink, P.D.A., Kulkarni, A.V., Mayewski, P.A., Nepal, S., Pacheco, P., Painter, T.H., Pellicciotti, F., Rajaram, H., Rupper, S., Sinisalo, A., Shrestha, A.B., Viviroli, D., Wada, Y., Xiao, C., Yao, T., Baillie, J.E.M., 2020. Importance and vulnerability of the world's water towers. Nature 577, 364–369. https://doi.org/10.1038/s41586-019-1822-y

Kabe, M., Rezaei, M., 2025. Impact of hydrogeological regime changes on the Bakhtegan-Tashk lake system under groundwater overextraction. Journal of Hydrology: Regional Studies 62, 102953. https://doi.org/10.1016/j.ejrh.2025.102953

Kiani, T., Ramesht, M.H., Maleki, A., Safakish, F., 2017. Analyzing the Impacts of Climate Change on Water Level Fluctuations of Tashk and Bakhtegan Lakes and Its Role in Environmental Sustainability. OJE 07, 158–178. https://doi.org/10.4236/oje.2017.72012

Kim, H.H., 1992. Urban heat island. International Journal of Remote Sensing 13, 2319–2336. https://doi.org/10.1080/01431169208904271

Lehner, B., Beames, P., Mulligan, M., Zarfl, C., De Felice, L., Van Soesbergen, A., Thieme, M., Garcia De Leaniz, C., Anand, M., Belletti, B., Brauman, K.A., Januchowski-Hartley, S.R., Lyon, K., Mandle, L., Mazany-Wright, N., Messager, M.L., Pavelsky, T., Pekel, J.-F., Wang, J., Wen, Q., Wishart, M., Xing, T., Yang, X., Higgins, J., 2024. The Global Dam Watch database of river barrier and reservoir information for large-scale applications. Sci Data 11, 1069. https://doi.org/10.1038/s41597-024-03752-9

Lehner, B., Grill, G., 2013. Global river hydrography and network routing: baseline data and new approaches to study the world's large river systems. Hydrological Processes 27, 2171–2186. https://doi.org/10.1002/hyp.9740

Madani, K., 2014. Water management in Iran: what is causing the looming crisis? J Environ Stud Sci 4, 315–328. https://doi.org/10.1007/s13412-014-0182-z

Messager, M.L., Lehner, B., Grill, G., Nedeva, I., Schmitt, O., 2016. Estimating the volume and age of water stored in global lakes using a geo-statistical approach. Nat Commun 7, 13603. https://doi.org/10.1038/ncomms13603

Mirmousavi, S.H., 2024. Analysis of drought effects on water level changes in Bakhtegan, Tashk and Maharloo lakes. Sepehr Scientific-Research Quarterly of Geographical Information, 33(130), pp.139–159. doi:10.22131/sepehr.2024.2004008.2983.

https://doi.org/10.5194/egusphere-2026-6728
Preprint. Discussion started: 11 November 2026
© Author(s) 2026. CC BY 4.0 License.

Mohammadibigedli, S., Malmasi, S., Zaeimdar, M. and Zamanpour, M., 2022. Assessment of climate change in the Tashk watershed using modelling and prediction of possible scenarios. Watershed Management Research Journal, 35(2), pp.88–100. doi:10.22092/WMRJ.2021.354855.1417.

Mozafari, M., Hosseini, Z., Fijani, E., Eskandari, R., Siahpoush, S., Ghader, F., 2022. Effects of climate change and human activity on lake drying in Bakhtegan Basin, southwest Iran. Sustain. Water Resour. Manag. 8, 109. https://doi.org/10.1007/s40899-022-00707-z

Muñoz-Sabater, J., Dutra, E., Agustí-Panareda, A., Albergel, C., Arduini, G., Balsamo, G., Boussetta, S., Choulga, M., Harrigan, S., Hersbach, H., Martens, B., Miralles, D.G., Piles, M., Rodríguez-Fernández, N.J., Zsoter, E., Buontempo, C., Thépaut, J.-N., 2021. ERA5-Land: a state-of-the-art global reanalysis dataset for land applications. Earth Syst. Sci. Data 13, 4349–4383. https://doi.org/10.5194/essd-13-4349-2021

Nasiri, A., Khosravian, M., Zandi, R., Entezari, A., Baaghide, M., 2023. Analysis of physical changes in Fars province water zones related to climatic parameters using remote sensing, Bakhtegan, Tashk, Iran. The Egyptian Journal of Remote Sensing and Space Sciences 26, 851–861. https://doi.org/10.1016/j.ejrs.2023.09.003

Pekel, J.-F., Cottam, A., Gorelick, N., Belward, A.S., 2016. High-resolution mapping of global surface water and its long-term changes. Nature 540, 418–422. https://doi.org/10.1038/nature20584

Ramsar Convention Secretariat. (2016). *An introduction to the Convention on Wetlands* (5th ed.). Ramsar Convention Secretariat.

Rashki, A., Middleton, N. J., & Goudie, A. S. (2021). Dust storms in Iran—Distribution, causes, frequencies and impacts. Aeolian Research, 48, Article 100655. https://doi.org/10.1016/j.aeolia.2020.100655

Sajedipour, S., Zarei, H., Oryan, S., 2017. Estimation of environmental water requirements via an ecological approach: A case study of Bakhtegan Lake, Iran. Ecological Engineering 100, 246–255. https://doi.org/10.1016/j.ecoleng.2016.12.023

Sayyah-Jahromi and Hatami (2023), n.d. Bakhtegan: the second-largest lake in Iran 8, 67–80. https://doi.org/DOI:10.22092/irn.2023.362933.1536

Shadkam, S., Ludwig, F., Van Oel, P., Kirmit, Ç., Kabat, P., 2016. Impacts of climate change and water resources development on the declining inflow into Iran's Urmia Lake. Journal of Great Lakes Research 42, 942–952. https://doi.org/10.1016/j.jglr.2016.07.033

Shokri, N., Hassani, A., Sahimi, M., 2024. Multi-Scale Soil Salinization Dynamics From Global to Pore Scale: A Review. Reviews of Geophysics 62, e2023RG000804. https://doi.org/10.1029/2023RG000804

Sun, Z., Wang, S., Yan, X., Li, Y., Zhou, L., Cheng, W., Ren, Z., 2026. Dataset of typical terminal lake and surrounding oasis outlines in arid/semi-arid endorheic basins based on remote sensing data. Sci Data. https://doi.org/10.1038/s41597-026-06671-z

Tao, S., Fang, J., Ma, S., Cai, Q., Xiong, X., Tian, D., Zhao, X., Fang, L., Zhang, H., Zhu, J., Zhao, S., 2020. Changes in China's lakes: climate and human impacts. National Science Review 7, 132–140. https://doi.org/10.1093/nsr/nwz103

Torabi Haghighi, A., & Kløve, B. (2017). Design of environmental flow regimes to maintain lakes and wetlands in regions with high seasonal irrigation demand. Ecological Engineering, 100, 120–129. https://doi.org/10.1016/j.ecoleng.2016.12.015

Turner, B.L., Lambin, E.F., Reenberg, A., 2007. The emergence of land change science for global environmental change and sustainability. Proc. Natl. Acad. Sci. U.S.A. 104, 20666–20671. https://doi.org/10.1073/pnas.0704119104

Vahidipour, M., Raeisi, E., Van Der Zee, S.E.A.T.M., 2021. Active saltwater intrusion of shrinking Bakhtegan -Thask Lakes in South Iran threatens the freshwater resources of coastal aquifers. Journal of Hydrology: Regional Studies 34, 100790. https://doi.org/10.1016/j.ejrh.2021.100790

https://doi.org/10.5194/egusphere-2026-6728
Preprint. Discussion started: 11 November 2026
© Author(s) 2026. CC BY 4.0 License.



Wulder, M.A., Loveland, T.R., Roy, D.P., Crawford, C.J., Masek, J.G., Woodcock, C.E., Allen, R.G., Anderson, M.C., Belward, A.S., Cohen, W.B., Dwyer, J., Erb, A., Gao, F., Griffiths, P., Helder, D., Hermosilla, T., Hipple, J.D., Hostert, P., Hughes, M.J., Huntington, J., Johnson, D.M., Kennedy, R., Kilic, A., Li, Z., Lymburner, L., McCorkel, J., Pahlevan, N., Scambos, T.A., Schaaf, C., Schott, J.R., Sheng, Y., Storey, J., Vermote, E., Vogelmann, J., White, J.C., Wynne, R.H., Zhu, Z., 2019. Current status of Landsat program, science, and applications. Remote Sensing of Environment 225, 127–147. https://doi.org/10.1016/j.rse.2019.02.015

Zhang, X., Zhao, T., Xu, H., Liu, W., Wang, J., Chen, X., Liu, L., 2024. GLC_FCS30D: the first global 30 m land-cover dynamics monitoring product with a fine classification system for the period from 1985 to 2022 generated using dense-time-series Landsat imagery and the continuous change-detection method. Earth Syst. Sci. Data 16, 1353–1381. https://doi.org/10.5194/essd-16-1353-2024